Effects of dephasing in molecular transport junctions using atomistic first principles

Jesse Maassen,* Ferdows Zahid, and Hong Guo
Centre for the Physics of Materials and Department of Physics, McGill University, Montreal, Quebec, Canada H3A 2T8
(Received 7 April 2009; revised manuscript received 26 June 2009; published 24 September 2009)

We report a theoretical investigation of dephasing effects to quantum transport properties of molecular junctions. The quantum transport analysis is done by density functional theory carried out within the nonequilibrium Green's function framework, and the dephasing effect is modeled within the Büttiker-probe approach. We observe two distinct behaviors in the three systems we studied: either an increase or a decrease in electronic conduction with dephasing. For a 1,4-benzenedithiol molecule and an atomic gold chain, where the conducting molecular levels are located away from the Fermi level, conduction is seen to increase due to reduced destructive interference resulting from the Büttiker probe. On the other hand, for a very thin Al nanowire we find that backscattering dominates over the phase-randomization and the current decreases with dephasing. The resistance follows Ohm's law while the resistivity scales linearly with the scattering rate. Finally, a comparison between the Büttiker-probe model and a more microscopic dephasing model shows nearly identical transport characteristics. From a computational point of view, the Büttiker-probe model has an order of magnitude speed up.

DOI: 10.1103/PhysRevB.80.125423 PACS number(s): 85.65.+h, 31.15.A−, 73.63.−b, 72.20.Dp

I. INTRODUCTION

An important issue in the field of molecular electronics is the influence of phase-relaxing scattering, i.e., dephasing, on charge transport characteristics of molecular systems. A main dephasing mechanism arises from the coupling of quantized molecular vibrational modes with the electronic scattering states,[1] which is often referred to as electron-phonon (*e-ph*) interaction in molecular transport junctions. Recently, *e-ph* interactions have received attention both experimentally[1–8] and theoretically[9–14] for systems where a single molecule is sandwiched between two metallic leads. Typical examples of molecules used in theory and experiments include alkanethiol molecular wires, benzenedithiol molecules, and atomic gold chains, whereas the leads are usually made of gold or aluminum. Experimentally, *e-ph* interactions can be inferred by measuring single molecule vibrational spectrum using inelastic tunneling spectroscopy.[1,2,5] This roughly corresponds to analyzing positions of the peaks in the second derivative (d^2I/d^2V) of a current (I)-voltage (V) curve, where the voltages at the peaks coincide with energies of the phonons, i.e., $\hbar\omega = e|V^{peak}|$. For a theoretical analysis of the *e-ph* interaction, the state of the art technique is to employ density functional theory (DFT) with the nonequilibrium Green's function (NEGF) formalism where the *e-ph* interactions are included through a self-energy term which must all be solved self-consistently.[9,10] In order to quantitatively calculate the *nonequilibrium e-ph* scattering in molecular devices, the atomic structure must be relaxed for every bias potential in calculating the *e-ph* coupling matrix and the vibrational spectrum,[9] which is computationally very time-consuming and can become almost intractable for molecular transport junctions involving even only a modest number of atoms. For qualitative and semiquantitative analysis of effects of inelastic scattering induced dephasing, it is therefore advantageous to start from less expensive models.

One such model for dephasing was originally proposed by Büttiker over twenty years ago.[15,16] The basic idea is to introduce a fictitious voltage probe into a coherent system, which in turn induces a phase-breaking process. Since the net current in the fictitious voltage probe should be zero, all electrons scattered into the fictitious probe are emitted back into the device with no definite phase relation to the incident coherent electrons, i.e., phase-memory is lost through such a scattering process.[17] To implement this model in a practical calculation, one connects fictitious probes to every spatial site in the device, and adjusts the electrochemical potential μ such that no net current flows through the fictitious probes. Because of its simplicity and appealing physical intuition, the Büttiker-probe model has been widely used in mesoscopic physics.[18–28]

The purpose of this paper is to examine the dephasing effects in realistic molecular device structures by using the phenomenological Büttiker-probe model within an *ab initio* transport formalism. Nozaki *et al.* applied this dephasing model to several molecular junctions[28] where the equilibrium transport properties were calculated using the extended Hückel theory. In this work, we implement the Büttiker-probe model into a NEGF-DFT-based *ab initio* nonequilibrium transport formalism.[29,30] Then, we apply the model to study the following three molecular systems: (i) a 1,4-benenedithiol (BDT) molecule sandwiched between two Al(001) leads (Al-BDT-Al), (ii) an atomic gold chain connected to Au(001) leads, i.e., a gold quantum point contact (gold QPC), and (iii) a very thin Al(001) nanowire (AlNW). In the Büttiker-probe model, the dephasing strength (electron-phonon coupling) is controlled by an adjustable phenomenological parameter γ. We present the theoretical I-V characteristics of the above three systems for different values of γ. For the first two systems, we notice an increase in current with γ whereas in the case of AlNW an opposite behavior is observed. The resistance and the resistivity data are presented for AlNW with results showing classical behavior. Finally, a comparison is made between the Büttiker-probe model and another more recent model for dephasing, which has been proposed by Golizadeh-Mojarad and Datta.[27]

Both dephasing models show almost identical *I-V* characteristics.

The rest of the paper is organized as follows: in Sec. II, we present our theoretical methods elaborating on the implementation of the Büttiker-probe model. All the results are presented in Sec. III. We conclude with a short summary in Sec. IV.

II. THEORETICAL METHOD

Within the NEGF-DFT formalism, the electronic structure of the system is determined by DFT where the density matrix is calculated self-consistently using the NEGF framework.[17,29] We refer interested readers to Refs. 29 and 30 for implementation details of the NEGF-DFT formalism and here we focus on extending the Büttiker-probe model into the NEGF-DFT.

The dephasing effect due to the Büttiker probes is introduced through a scattering self-energy term Σ_B^r (subscript B stands for Büttiker probe) as follows:

$$\Sigma_B^r = -\frac{i}{2}\gamma S$$

$$G^r(E) = [ES - \mathcal{H} - \Sigma_L^r(E) - \Sigma_R^r(E) - \Sigma_B^r]^{-1}, \tag{1}$$

where γ is the dephasing parameter of the Büttiker-probe model, G^r is the retarded nonequilibrium Green's function, $\mathcal{H}$ is the Hamiltonian matrix, S is the overlap matrix, and $\Sigma_{L,R}^r$ are the retarded self-energies of the left and right lead. The scattering self-energy Σ_B^r is obtained by summing up the self-energy term Σ_p^r of each fictitious Büttiker probe where $p=1,2,\ldots,N$ with N being the total number of fictitious probes, which is equal to the number of atomic orbitals. This form of Σ_B^r is equivalent to each atomic orbital (in orthogonal representation) being connected to a fictitious probe with a coupling strength γ. Note that Σ_B^r is omitted from the NEGF-DFT self-consistent iteration which determines the Hamiltonian of the open device, as a test calculation showed insignificant differences in the total density of states.

The general expression for current I at any probe m (including the left and the right lead) is given by[31–33]

$$I_m = \int \tilde{i}_m(E)dE$$

$$\tilde{i}_m(E) = \frac{2e}{h}\sum_n T_{mn}(E)[f_m(E) - f_n(E)]$$

$$T_{mn} = \mathrm{Tr}[\Gamma_m G^r \Gamma_n G^a]$$

$$\Gamma_m = i(\Sigma_m^r - \Sigma_m^a), \tag{2}$$

where $m,n \in [p,L,R]$, $G^a=(G^r)^\dagger$, and $\Sigma_m^a=(\Sigma_m^r)^\dagger$, T_{mn} is the transmission coefficient between probes m and n, Γ_m is the linewidth function at probe m, $\tilde{i}_m$ is the current density that is essentially equivalent to an effective transmission at nonequilibrium, and $f_m(E)=f(E-\mu_m)$ is the Fermi-Dirac distribution with μ_m being the electrochemical potential of lead m.

In the above expression for current, the unknown quantities are the electrochemical potentials μ_p of the fictitious probes that can be obtained by applying the condition of zero current (essential for current conservation) in every Büttiker probe. Since the current in each Büttiker probe depends on the electrochemical potentials of all other probes, one must solve the condition $I_p=\int \tilde{i}_p(E)dE=0$ simultaneously for all $p \in [1,N]$, which implies solving N nonlinear coupled equations. This cannot be done analytically due to the energy integral in Eq. (2). An alternative scheme for current conservation is to set the integrand itself to zero, i.e., $\tilde{i}_p(E)=0$ at every energy. This is analytically solvable and greatly reduces the computation time. Although this solution omits the inelastic effects, it *does* capture the phase-breaking scattering. In this study, our main purpose is to introduce a *practical* dephasing model into our *ab initio* transport formalism, we therefore choose the energy conserved (elastic) option for calculating μ_p. For further details on these two solution schemes, see Ref. 25.

In the elastic scheme, the electrochemical potentials μ_p can be easily obtained by solving a linear matrix equation of the form: $A\cdot\mathbf{f}=\mathbf{b}$, where A is a square matrix of dimension N and $\mathbf{f}$ and $\mathbf{b}$ are vectors of length N. The matrix elements are given by

$$A_{pp} = \sum_{q=1,q\neq p}^{N} T_{pq} + T_{pL} + T_{pR}$$

$$A_{pq} = -T_{pq}$$

$$\mathbf{b}_p = T_{pL}f_L(E) + T_{pR}f_R(E)$$

$$\mathbf{f}_p = f_p(E), \tag{3}$$

where all the elements of the matrix A and the vector $\mathbf{b}$ are known. We obtain the values of μ_p at every energy by inverting the matrix A and solving for $\mathbf{f}$ with $\mathbf{f}=A^{-1}\mathbf{b}$. Similar solutions for obtaining μ_p have been presented in Refs. 18 and 25. With the values of μ_p we can then calculate the terminal current from Eq. (2). Note that this scheme is general and can be applied to any system.

In addition to phase randomization, the Büttiker-probe model also introduces extra resistance in the system by relaxing the momentum of the electrons, i.e., backscattering. We believe that a "momentum relaxing" dephasing model is appropriate for systems where the dominant scattering source does not conserve electronic momentum, such as *e-ph* interaction which is important in molecular conductors. Recently, a new momentum relaxing *elastic* dephasing model has been proposed by Golizadeh-Mojarad and Datta[27] (it will be referred to as Datta model from hereafter) which is derived from *e-ph* scattering and can thus be considered as more directly connected to microscopic scattering processes. In the Datta model, within the nonorthogonal atomic orbital representation, the retarted self-energy (Σ_D^r) and the lesser self-energy ($\Sigma_D^<$) due to scattering are given by

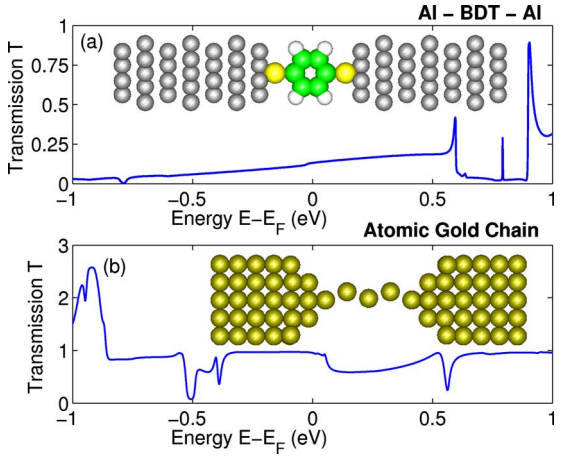

FIG. 1. (Color online) Transmission coefficient as a function of energy for Al-BDT-Al (a) and gold QPC (b) at equilibrium without any dephasing. The corresponding relaxed atomic structures of the two systems are shown in the insets.

$$\Sigma_D^r = d \cdot SG^r S$$

$$\Sigma_D^< = d \cdot SG^< S, \tag{4}$$

where the proportionality constant d is an adjustable parameter of the Datta model, $G^<$ is the lesser nonequilibrium Green's function and the subscript D stands for Datta model. Both Σ_D^r and $\Sigma_D^<$ are calculated self-consistently which makes the Datta model more computationally expensive as compared to the Büttiker-probe model. For further details on the Datta model see Ref. 27.

The *elastic* Büttiker-probe model as discussed above is used to study the following three systems: (i) Al-BDT-Al, (ii) gold QPC, and (iii) a very thin AlNW. In all cases, the leads extend to $z=\pm\infty$ along the transport direction z and have a finite cross section. For the first two systems, the atomic structure is fully relaxed using the SIESTA DFT package[34] with the outermost layers of the lead atoms fixed at their bulk positions. The bulk value of the lattice constant (4.05 Å) is used for the Al nanowire. After the atomic structures are relaxed, we carry out the self-consistent NEGF-DFT calculation within the local density approximation employing standard norm-conserving pseudopotentials[35] and double-ζ polarized basis sets for all atoms. Note that the quantities calculated self-consistently are the device Hamiltonian $\mathcal{H}$ (by NEGF-DFT) and the Datta model self-energy $\Sigma_D^{r,<}$. All the calculations are performed at a temperature of 5 K. For the nonequilibrium calculations the bias polarity is defined as follows: $\mu_L=E_F$ and $\mu_R=E_F+|e|V$ where E_F is the Fermi energy and V is the applied bias.

III. RESULTS AND DISCUSSION

In order to get a clear understanding of the dephasing effects, it is useful to first study the transport properties of the fully coherent systems. Figure 1(a) shows the transmission (T) versus energy (E) for the BDT molecule at equilibrium without any dephasing. We see that around E_F the transmission is very flat with an average value of around 0.12. There are several peaks with higher transmission starting roughly 0.6 eV above E_F. By comparing the density of states of the device and of the isolated leads (not presented here) to T, it is clear that the states near E_F are lead dominated and that the peaks at 0.60 and 0.90 eV result from Van Hove singularities in the leads. A scattering state analysis (i.e., a projection of the scattering states onto the molecular eigenstates, for further details see Ref. 36) shows that the peak at 0.79 eV is due to a molecular eigenstate (specifically, the lowest unoccupied molecular orbital+3). Moreover, the presence of potential barriers at the metal-molecule interfaces also contribute to the low average transmission near E_F. The transmission properties of gold QPC [see Fig. 1(b)] is also relatively flat around E_F with several intermittent plateaulike features. Due to the absence of tunneling barriers at the interfaces, the transmission for gold QPC is much higher at E_F. A transmission value of $T\sim 1$ indicates that the conducting states near E_F are mostly composed of s-type orbitals that form a single conducting channel. Both sets of results [Figs. 1(a) and 1(b)] are reasonably consistent with the available experimental data[37,38] and other theoretical studies[39–44] on these two molecular systems.

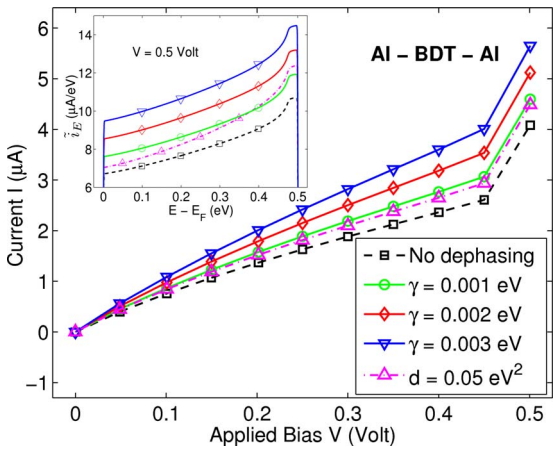

FIG. 2. (Color online) I-V curves for the Al-BDT-Al system using two different dephasing models: Büttiker probe and Datta model (purple up-triangle) (Ref. 27) where γ and d are the corresponding adjustable parameters of the two models, respectively. Inset: Current density as a function of energy at applied bias V =0.5 V.

The current-voltage (I-V) characteristics of the Al-BDT-Al and gold QPC systems for different values of the Büttiker probe dephasing parameter γ are presented in Figs. 2 and 3, respectively. For both systems we observe a linear increase in current with dephasing. The increase in current indicates the dominance of the phase-relaxation effects over backscattering. As can be understood from a simple dephasing picture, reduced destructive interference due to phase-relaxation can enhance conduction around E_F (located away from the conducting molecular levels as seen in Fig. 1) and thus increase the current. Note that we assume phase-randomization results from e-ph interaction which is important in molecular electronics[1] and can lead to significant effects to quantum transport.[45] Thus, the values of γ (ranging

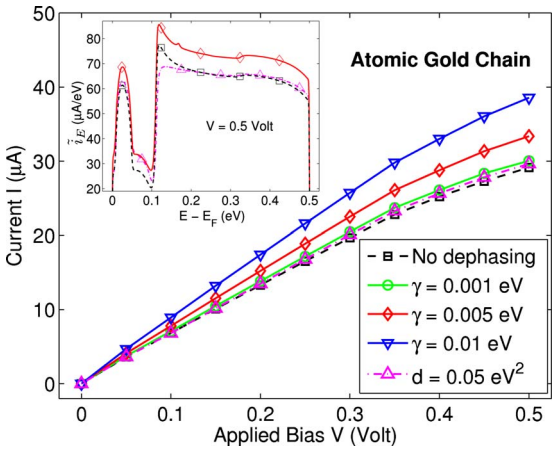

FIG. 3. (Color online) *I-V* plot for the gold QPC using two different dephasing models: Büttiker probe and Datta model (purple up-triangle) (Ref. 27) where γ and d are the corresponding adjustable parameters of the two models, respectively. Inset: Current density as a function of energy at applied bias $V=0.5$ V.

from $\gamma=0.001$ to 0.003 eV) are chosen from the *e-ph* coupling calculated for the BDT system from an atomistic *ab initio* technique.[9] Their results showed that the elastic/inelastic *e-ph* coupling energy is roughly a few meV, which corresponds to the energy range for γ. This choice was motivated by setting the dephasing rate equal to the *e-ph* scattering rate which are each related to γ and the *e-ph* coupling energy, respectively. Since the number of phonon modes participating in electronic transport, and hence the *e-ph* scattering rate, varies with temperature and voltage, γ is in principle a function of these external parameters. Here, for simplicity, we take the Büttiker dephasing scheme to be a single parameter model provided by γ which can be considered as the average inelastic broadening parameter. In particular, here we used similar values of γ for the gold QPC system. A comparison of the Büttiker probe with the Datta dephasing model is also presented in both Figs. 2 and 3. It shows that almost identical *I-V* characteristics can be obtained with the Datta model for a particular value of the d parameter. Note that the computation speed is approximately an order of magnitude higher while using the Büttiker-probe model.

In the insets of Figs. 2 and 3, we show the current density ($\tilde{i}_E$) versus energy at $V=0.5$ V for the respective systems. As expected, for the energy independent Büttiker-probe model we do not observe any features in the $\tilde{i}_E$ versus E plots apart from a constant shift with the γ parameter. On the other hand, nonlinear energy dependent features are present in the current density with the Datta model. For gold QPC with the Datta model (see the inset of Fig. 3) the effective transmission actually decreases over a short range in the energy window (between 0.11 to 0.22 eV) which could be due to the enhanced backscattering from the off diagonal elements of the full matrix of the Datta self-energy Σ_D^r, as opposed to the simple diagonal form of the Büttiker probe self-energy Σ_B^r. In the Datta model the self-energy Σ_D^r is proportional to the density of states which is a function of energy [see Eq. (4)]. Hence, the change to the current density, resulting from the Datta model, shows a nonlinear behavior with energy.

Since the Büttiker probe is a phenomenological model, it is somewhat difficult to establish a rigorous relationship between the Büttiker-probe model and the Datta model. Nevertheless, by comparing the dephasing rates of the two models an approximate relation between the two parameters γ and d can be deduced. In the nonorthogonal representation, the dephasing rate can be defined as

$$\nu = \frac{\mathrm{Tr}(S^{-1}\Gamma_s)}{h}, \tag{5}$$

where Γ_s is the linewidth function matrix due to scattering such that $s=B,D$. Then, from Eqs. (1) and (5), we obtain the dephasing rate for the Büttiker-probe model

$$\nu_B = \frac{N\gamma}{h}, \tag{6}$$

where N is the number of orbitals in the scattering molecule. Note that ν_B is energy independent. Similarly, the dephasing rate for the Datta model can be obtained from Eqs. (4) and (5) as

$$\nu_D = \frac{2\pi}{h} d\bar{D}$$

$$\bar{D} = \int_0^{eV} \frac{\mathrm{Tr}[A(E)S]}{2\pi \cdot eV} dE$$

$$A(E) = i(G^r - G^a), \tag{7}$$

where $\bar{D}$ is the energy-averaged density of states of the scattering molecule. By setting these two dephasing rates equal to each other, we obtain the following simple relation between the parameters γ and d:

$$\gamma = \frac{2\pi}{N} \bar{D} d. \tag{8}$$

This simple approximate relation should provide reasonable results as long as the off diagonal elements of Γ_D matrix do not contribute significantly to the conduction. From Eq. (8) with $d=0.05$ eV^2, $\bar{D}=0.4815$ eV^{-1}, and $N=124$, we obtain a value of $\gamma=0.0012$ eV for the BDT molecule. From the *I-V* curve (see Fig. 2), a value of $\gamma=0.0012$ eV fits reasonably well to the points calculated using $d=0.05$ eV^2, indicating the above correspondence between parameters of the two dephasing models to be reasonable.

Next, we study the effects of dephasing on a very thin Al (001) nanowire (AlNW) using the Büttiker-probe model within the NEGF-DFT formalism. The atomic structure of the nanowire is shown in the inset of Fig. 4. It is a two probe device with a specific cross section of area $A=6.261 \times 10^{-19}$ m^2. For all our calculations, the cross section of the nanowire is kept constant whereas the length has been varied. In Fig. 4, we present the current density as a function of

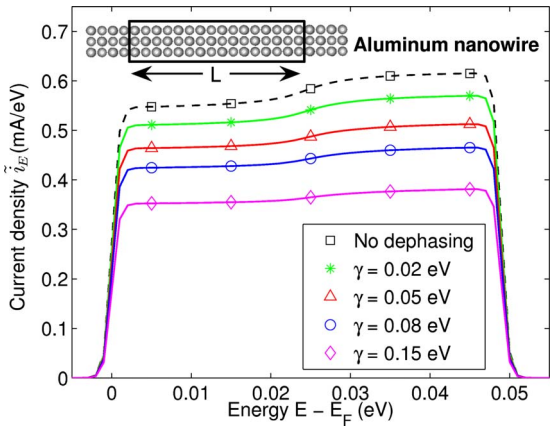

FIG. 4. (Color online) Current density as a function of energy for AlNW at V=0.5 V for different values of γ, where γ is the adjustable parameter of the Büttiker-probe model. The atomic structure of the AlNW used in our calculations is shown in the inset where the length of the nanowire is L=3.44 nm, i.e., 16 atomic layers.

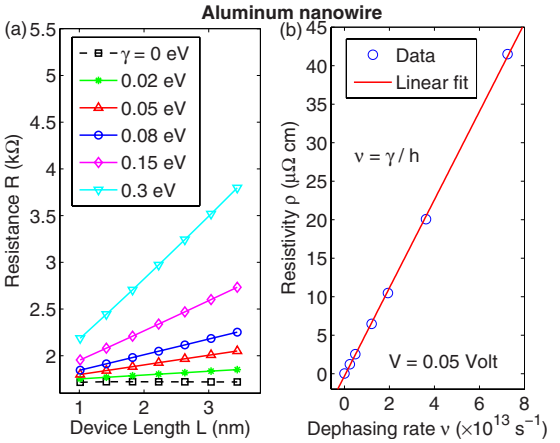

FIG. 5. (Color online) (a) Resistance as a function of length of the AlNW for different values of γ; (b) Resistivity as a function of the dephasing rate ($\nu = \gamma/h$). All the data are calculated at the applied bias V=0.05 V.

energy for different values of γ at 0.05 V applied bias. We notice that the current is going down with the increasing dephasing strength, which is exactly the opposite behavior observed for the molecular systems: Al-BDT-Al (Fig. 2) and gold QPC (Fig. 3). The increase in the resistance is mainly due to backscattering effects, which is introduced in the system by the Büttiker probes. We believe that the backscattering effects become more dominant in the metallic system AlNW which has perfect interfaces with the leads at both ends as opposed to the molecular systems of Al-BDT-Al and gold QPC. The step in the current density near $E-E_F$ =0.024 eV is due to the presence of an extra conducting mode in the bias window at that energy. As the transmission per mode goes down with the higher values of γ, the step in the current density becomes less apparent.

In Fig. 5(a), we present the resistance (R) as a function of length (L) of the AlNW for the different values of γ at the applied bias of V=0.05 V. We observe that the resistance increases linearly with length following Ohm's law. Without dephasing (i.e., with γ=0) the resistance is independent of the length with a constant value of 1.72 kΩ) which is the so-called contact resistance.[17] In a nonequilibrium situation when $V \neq 0$, the contact resistance can be written as R_C =12.9/$\bar{T}$ kΩ where $\bar{T}$ is the average transmission over the energy range $\mu_L < E < \mu_R$. From the above relation we obtain the value of $\bar{T}$ as 7.5 which is, indeed, the average number of bands or channels within the bias range as obtained from the band structure calculations of AlNW (not presented here). From the slope of the R versus L curves we can obtain the resistivity ρ as a function of the dephasing rate ν (where $\nu = \gamma/h$). The results are plotted in Fig. 5(b) which shows a linear behavior, similar to that predicted by the Drude theory of metals.[46] We note in passing that dephasing is a complicated effect influenced by inelastic scattering events. So far we motivated our choice of the γ parameter by *e-ph* interactions. For metallic wires, *e-ph* scattering sets an inelastic mean free path typically a few to tens of nanometers. Dephasing effect is expected to operate when system sizes approach this scale.

IV. CONCLUSION

In conclusion, we investigated effects of dephasing on electron transport in molecular systems by including the Büttiker-probe model into our first principles based atomistic NEGF-DFT quantum transport formalism. The results showed two types of distinct behaviors: (i) for the "low-conductance" systems (namely, Al-BDT-Al and gold QPC) where the conducting molecular eigenstates are located away from E_F, dephasing effects minimize the destructive interference effects and increase the conduction; (ii) for the "high-conductance" system (namely, AlNW), we observe the opposite effect where backscattering dominates over interference effects resulting in an increase in the resistance and the resistivity scales down linearly with the scattering rate similarly to the Drude theory of metals. Finally, the *elastic* Büttiker-probe model is compared to the Datta dephasing model and it shows moderate differences in the current density while the *I-V* characteristics are nearly identical. With a computation speed of roughly an order of magnitude higher, the Büttiker-probe model is found to be a very practical and efficient phenomenological method to qualitatively study phase-breaking phenomena in molecular conductors.

ACKNOWLEDGMENTS

We would like to thank Zhanyu Ning, Tao Ji, and Yu Zhu for many helpful discussions on the dephasing physics and the NEGF-DFT calculations. This work is supported by the FQRNT of Québec, NSERC of Canada, and CIFAR.

*maassenj@physics.mcgill.ca

[1] M. Galperin, M. A. Ratner, and A. Nitzan, J. Phys.: Condens. Matter **19**, 103201 (2007).
[2] B. C. Stipe, M. A. Rezaei, and W. Ho, Science **280**, 1732 (1998).
[3] N. Agraït, C. Untiedt, G. Rubio-Bollinger, and S. Vieira, Phys. Rev. Lett. **88**, 216803 (2002).
[4] W. Ho, J. Chem. Phys. **117**, 11033 (2002).
[5] W. Wang, T. Lee, I. Kretzschmar, and M. A. Reed, Nano Lett. **4**, 643 (2004).
[6] W. Wang, T. Lee, and M. A. Reed, J. Phys. Chem. B **108**, 18398 (2004).
[7] J. G. Kushmerick, J. Lazorcik, C. H. Patterson, R. Shashidhar, D. S. Seferos, and G. C. Bazan, Nano Lett. **4**, 639 (2004).
[8] Y. Selzer, L. Cai, M. A. Cabassi, Y. Yao, J. M. Tour, T. H. Mayer, and D. L. Allara, Nano Lett. **5**, 61 (2005).
[9] N. Sergueev, D. Roubtsov, and H. Guo, Phys. Rev. Lett. **95**, 146803 (2005).
[10] N. Sergueev, A. A. Demkov, and H. Guo, Phys. Rev. B **75**, 233418 (2007).
[11] T. Frederiksen, M. Brandbyge, N. Lorente, and A.-P. Jauho, Phys. Rev. Lett. **93**, 256601 (2004).
[12] M. Paulsson, T. Frederiksen, H. Ueba, N. Lorente, and M. Brandbyge, Phys. Rev. Lett. **100**, 226604 (2008).
[13] A. Pecchia, G. Romano, and A. Di Carlo, Phys. Rev. B **75**, 035401 (2007).
[14] S. Roche, J. Jiang, F. Triozon, and R. Saito, Phys. Rev. Lett. **95**, 076803 (2005).
[15] M. Büttiker, Phys. Rev. B **33**, 3020 (1986).
[16] M. Büttiker, IBM J. Res. Dev. **32**, 63 (1988).
[17] S. Datta, *Electronic Transport in Mesoscopic Systems* (Cambridge University Press, New York, 1995).
[18] J. L. D'Amato and H. M. Pastawski, Phys. Rev. B **41**, 7411 (1990).
[19] T. P. Pareek, S. K. Joshi, and A. M. Jayannavar, Phys. Rev. B **57**, 8809 (1998).
[20] N. A. Mortensen, A.-P. Jauho, and K. Flensberg, Superlattices Microstruct. **28**, 67 (2000).
[21] J. Shi, Z. Ma and X. C. Xie, Phys. Rev. B **63**, 201311(R) (2001).
[22] X.-Q. Li and Y. Yan, Appl. Phys. Lett. **79**, 2190 (2001).
[23] X.-Q. Li and Y. Yan, Phys. Rev. B **65**, 155326 (2002).
[24] Z. Ma, K. A. Chao, and G. He, Solid State Commun. **122**, 217 (2002).
[25] R. Venugopal, M. Paulsson, S. Goasguen, S. Datta, and M. S. Lundstrom, J. Appl. Phys. **93**, 5613 (2003).
[26] J. Wang, E. Polizzi, and M. Lundstrom, J. Appl. Phys. **96**, 2192 (2004).
[27] R. Golizadeh-Mojarad and S. Datta, Phys. Rev. B **75**, 081301(R) (2007).
[28] D. Nozaki, Y. Girard and K. Yoshizawa, J. Phys. Chem. C **112**, 17408 (2008).
[29] J. Taylor, H. Guo, and J. Wang, Phys. Rev. B **63**, 245407 (2001); **63**, 121104(R) (2001).
[30] D. Waldron, P. Haney, B. Larade, A. MacDonald, and H. Guo, Phys. Rev. Lett. **96**, 166804 (2006); D. Waldron, L. Liu, and H. Guo, Nanotechnology **18**, 424026 (2007).
[31] A.-P. Jauho, N. S. Wingreen, and Y. Meir, Phys. Rev. B **50**, 5528 (1994).
[32] S. Datta, *Quantum Transport: Atom to Transistor* (Cambridge University Press, Cambridge, England, 2005).
[33] Our starting point for arriving at Eq. (2) is $I_m = (2ie/h)\int \mathrm{Tr}\{\Gamma_m(E)\{G^<(E) + f_m(E)[G^r(E) - G^a(E)]\}\}dE$ (see Ref. 31), where $G^<$ is the nonequilibrium lesser Green's function. We rewrite $G^<$ in terms of $G^{r,a}$ using the Keldysh equation $G^< = G^r\Sigma^< G^a$, where $\Sigma_n^<(E) = if_n(E)\Gamma_n(E)$ for a lead labeled by n.
[34] J. Junquera, O. Paz, D. Sanchez-Portal, and E. Artacho, Phys. Rev. B **64**, 235111 (2001).
[35] D. R. Hamann, M. Schlüter, and C. Chiang, Phys. Rev. Lett. **43**, 1494 (1979).
[36] B. Larade, J. Taylor, Q. R. Zheng, H. Mehrez, P. Pomorski, and Hong Guo, Phys. Rev. B **64**, 195402 (2001).
[37] X. Xiao, B. Xu, and N. J. Tao, Nano Lett. **4**, 267 (2004).
[38] H. Ohnishi, Y. Kondo, and K. Takayanagi, Nature (London) **395**, 780 (1998).
[39] K. Stokbro, J. Taylor, M. Brandbyge, J. L. Mozos, and P. Ordejon, Comput. Mater. Sci. **27**, 151 (2003).
[40] F. Zahid, M. Paulsson, and S. Datta, in *Advanced Semiconductor and Organic Nano-Techniques*, edited by H. Morkoc (Academic Press, New York, 2003).
[41] S.-H. Ke, H. U. Baranger, and W. Yang, J. Chem. Phys. **123**, 114701 (2005).
[42] H. Mehrez, A. Wlasenko, B. Larade, J. Taylor, P. Grütter, and Hong Guo, Phys. Rev. B **65**, 195419 (2002).
[43] Y. J. Lee, M. Brandbyge, M. J. Puska, J. Taylor, K. Stokbro, and R. M. Nieminen, Phys. Rev. B **69**, 125409 (2004).
[44] P. S. Damle, A. W. Ghosh, and S. Datta, Phys. Rev. B **64**, 201403(R) (2001).
[45] L. E. F. Foa Torres and S. Roche, Phys. Rev. Lett. **97**, 076804 (2006).
[46] N. W. Ashcroft and N. D. Mermin, *Solid State Physics* (Holt, Rinehart, and Winston, New York, 1976).